Author Version: Geophys. Res. Lett., vol.37(17); 2010; 5 pp;
doi:10.1029/2010GL044347

Large Fault Fabric of the Ninetyeast Ridge Implies Near-Spreading Ridge Formation

W. W. Sager[1]*, C. F. Paul[1], K. S. Krishna[2], M. Pringle[3], A. E. Eisin[1,4], F. A. Frey[3], D. Gopala Rao[5], O. Levchenko[6]

[1]Department of Oceanography, Texas A&M University, College Station, TX 77843 USA
[2]National Institute of Oceanography, Council of Scientific and Industrial Research, Dona Paula, Goa 403004, India
[3]Department of Earth and Planetary Sciences, Massachusetts Institute of Technology, Cambridge, MA 02139 USA
[4]Now at Naval Oceanographic Office, Stennis Space Center, MS, 39522 USA
[5]Geology Department, Osmania University, Hyderabad AP 500 007, India
[6]Shirshov Institute of Oceanology, Russian Academy of Sciences, Moscow 117997, Russian Federation
*wsager@tamu.edu

Abstract

Ninetyeast Ridge (NER) is a linear volcanic ridge in the Indian Ocean thought to have formed by hotspot volcanism on the northward-drifting Indian plate. Geological data from the ridge are sparse, so its tectonic evolution is poorly known. We studied satellite-derived gravity data, seismic reflection profiles, and multibeam bathymetry to examine NER structure. Gravity data show that the ridge displays a series of nearly E-W trending lineations with average spacing ~0.4° (45 km). In seismic and bathymetry data, these lineations correlate with horsts and grabens that probably formed near the time of ridge emplacement. From their extensional nature and trends, we infer that these faulted structures formed near the spreading ridge that separated the Indian and Antarctic plates and their ubiquity implies the hotspot was never far from this spreading ridge.

1. Introduction

The NER is a linear, N-S oriented volcanic ridge located in the eastern Indian Ocean (Fig. 1). It extends ~5200 km from 30°S, where it intersects Broken Ridge, to ~17°N, where it is buried beneath the Bengal Fan [*Gopala Rao et al., 1997*]. Although many explanations have been given for the formation of the NER [*Royer et al., 1991*, and references therein], it is widely accepted that it formed from hotspot volcanism near the spreading ridge (Wharton Ridge) that separated the Indian and Antarctic plates, leaving a trail of volcanism on the former as it drifted northward during the Late Cretaceous and early Cenozoic [*Luyendyk, 1977; Royer et al., 1991*]. This interpretation is based on geochronology data, mainly from Deep Sea Drilling Project (DSDP) and Ocean Drilling Program (ODP) cores, which show a linear age progression from ~77 Myr at the north end to ~43 Myr near the south end [Fig. 2, *Duncan, 1991; Royer et al., 1991; Pringle et al., 2008*]. The NER ceased formation at anomaly 19 time (~41 Ma [*Gradstein et al., 2004*]) when a plate boundary reorganization stopped Wharton Ridge spreading, melded the Indian and Australian plates, and shifted spreading to the Southeast Indian Ridge (SEIR) [*Royer et al., 1991; Krishna et al., 1995*].

NER morphology is complex and varies along its length (Fig. 2). In the south, it is tall and nearly continuous, but the northern portion consists of a series of individual, large volcanoes. In between, NER is low with a mixture of linear segments and small seamounts. These differences are thought to have resulted from the changing distance of the hotspot from Wharton Ridge, with the northern NER forming off-ridge and the southern part, near-ridge [*Royer et al., 1991*]. The NER is too long to have formed simply by volcanism on the Indian plate because magnetic isochrons of the same age in adjacent basins cover ~11° less distance [*Krishna et al., 1995; 1999*]. Magnetic isochrons in Wharton Basin (east of NER) imply large spreading ridge jumps, which in turn imply that the NER incorporates sections of ridge formed on the Antarctic plate [*Royer et al., 1991; Pilipenko, 1996; Krishna et al., 1999*].

Faults have been observed on seismic profiles at various locations on NER [*Veevers, 1974; Curray and Munashinge, 1989; Pilipenko, 1996*], but no comprehensive picture of their extent and faulting history has been developed. Faults on the NER are little surprise because it formed at or near a spreading ridge and is currently at the nexus of diffuse intraplate deformation of the Indo-Australian plate (Fig. 1). Earthquakes occur on and around NER indicating ongoing deformation [see Fig. 2 in *Delescluse and Chamot-rooke, 2007*]. Most NER earthquake focal mechanisms indicate strike-slip strain along the northern part of the chain [*Petroy and Wiens, 1989*] and deformation modeling implies that the ridge is a weak zone and a boundary between different strain regimes to the east and west [*Delescluse and Chamot-Rooke, 2007*].

We examined three data sets that define structure within the NER. One is an update of the gravity field derived from satellite altimetry [*Sandwell and Smith, 2009*], showing larger tectonic features with a synoptic viewpoint. The other data are multibeam bathymetry and seismic reflection profiles collected during a cruise to NER (KNOX06RR, R/V *Roger Revelle*). Both data sets show structure with greater detail, but only in small areas. Altogether, these data indicate that the ridge is extensively faulted that the larger faults are ubiquitous and oriented mainly E-W.

2. Data and Methods

We examined ship bathymetry and seismic data to understand the pattern of tectonic features observed in satellite-derived gravity data [*Sandwell and Smith, 2009*]. Although the gravity grid interval is 1-minute, the actual resolution is not as fine because of upward continuation and the altimeter footprint. As a result, features with wavelengths less than ~15 km are significantly attenuated [*Sandwell and Smith, 2009*]. We interpreted the vertical gravity gradient because it highlights tectonic features [*Smith, 1998*]. In the oceans, the greatest density contrast is between water and rock, so the gravity gradient emphasizes seafloor variations.

Bathymetry data were collected continuously along ship tracks using a 12-kHz Kongsberg EM-120 multibeam echosounder. These data were processed using *MB-System* software, including deletion of bad soundings and construction of smooth bathymetry data grids. The EM-120 can make 191 soundings across a swath of 150°, which translates to ~7.5 times water depth. During KNOX06RR, rough seas frequently degraded outer soundings, often limiting swath width to 10-25 km. Greater areal coverage was achieved at seismic survey sites where ship tracks are closely-spaced.

Seismic profiles were shot at six survey sites (758, 216, NER2-NER3, 214, NER4, and 253; Fig. 2). Data were recorded using a Geometrics GeoEel streamer with six active sections, each 100 m in length with 8 hydrophone groups having an interval of 12.5 m. The seismic source was two identical generator/injector (GI) airguns (volumes 290 cm^3 and 677 cm^3). Data were recorded digitally at a sampling rate of 0.5 ms and processing was done with *ProMax* software, including geometry corrections, band-pass filtering, velocity analysis, common-depth-point gathers, normal-move-out correction, stacking, and time migration.

3. Observations

The gravity gradient (Fig. 2) shows prominent tectonic lineations over and around NER. A significant number of gravity lineations over NER have a roughly E-W orientation, giving the ridge a ladder-like appearance (Figs. 2B, 2C). The spacing of these features is irregular and ranges from ~0.2° (24 km) to ~0.9° (99 km) with an average of 0.4° (45 km). These lineations are most closely-spaced and consistent in trend over the NER south of 11°S. Between ~11° to 15°S, N-S oriented lineations signify steep flanks of the high ridge. At 26°S, prominent NE-SW oriented lineations extend southwest from the ridge. Some appear to connect with N-S fracture zone troughs east of NER, implying that the NE-SW features are fracture zone scars formed after the change in plate motion at anomaly 19 time.

Cruise KNOX06RR crossed many gravity lineations and ship data reveal a correspondence between gravity and bathymetric lineations. The largest E-W gravity lineations are caused by canyons, typically ~1-2 km deep. Although some have simple, steep sides (Fig. 2D), others have sides with terraced fault blocks that imply normal faulting. In many places, bathymetry data show ridge-and-trough morphology with a trend nearly perpendicular to the ridge (Fig. 3). This is especially true for NER south of ~4°S. Where KNOX06RR crossed a gravity lineation, negative gradient features correspond to troughs whereas positive gradient features result from igneous basement highs (Fig. 3). Seismic data imply that the troughs resulted from faulting that has been mainly extensional (i.e., grabens) whereas highs are fault-bounded horsts (Fig. 3). Although some have simple, steep sides, most grabens are compound features caused by a series of step-like faults (Fig. 3).

In the northern NER, the E-W pattern of gravity lineations appears less consistent (Fig. 2). Here many lineations result from steep seamount flanks and some have orientations other than E-W. Horsts and grabens are less common than in southern NER, but they are found in this part of the ridge and they incise seamount flanks or occur between seamounts. As in southern NER, they usually have a roughly E-W orientation. Moreover, gravity and bathymetry show that many seamount flanks in this part of the chain have trends or elongations with the same trend.

The similarity to southern NER tectonic trends suggests a common mechanism of formation despite the larger morphologic differences.

Seismic profiles show many faults within NER. Most faults offset igneous basement and extend a short distance into the overlying sediments (Fig. 3), implying that these faults were active as the ridge formed and for a time thereafter. Some faults penetrate the entire sediment column and offset the seafloor, implying recent motion. Faulting within NER is clearly complex and probably affected by ongoing intraplate deformation [*Krishna et al., 2009*]. Untangling the history of faulting on NER is beyond the scope of this report and we rely here on the observation that the features causing gravity gradient lineations are large horsts and grabens (Figs. 2, 3). Although seismic profiles often display numerous faults, most have small offsets (<100 m) and are therefore invisible to the satellite altimeter. Only the largest ridge and trough features cause satellite gravity lineations because smaller features are masked by upward continuation and the limited short-wavelength resolution of the satellite altimeter.

4. Discussion and Conclusions

The geophysical data analyzed here imply that the NER is heavily faulted. Clearly the ridge has had a complex tectonic history. It has already been hypothesized that NER evolution was complicated by ridge jumps [*Royer et al., 1991; Pilipenko, 1996; Krishna et al., 1999; Desa et al., 2009*] and this mechanism may explain the observed faulting as well as the discrepancy between the length of the NER and the observed linear age trend [*Pringle, 2008*].

An important question about the observed faults is whether they are constructional features or formed later by intraplate deformation. Two lines of evidence indicate that most of the large-offset faults are original. First, many grabens are filled with sediments and the greatest fill often correlates with basal volcaniclastic-rich layers in DSDP and ODP drill holes. These sediments appear to have been deposited soon after the formation of igneous basement [*Luyendyk, 1977*]. Older sediment fill implies that the larger troughs were initially formed at the time of ridge construction or shortly thereafter. Some of these faults are active and it is likely that intraplate deformation has reactivated existing faults here as it has in the adjacent Central Indian Basin [*Bull and Scrutton, 1990*].

The second observation is that fault extension and trends are consistent with a spreading ridge origin. Gravity gradient lineations are primarily oriented E-W and are relatively consistent in trend along the ridge. Horsts and grabens imply an extensional regime such as that associated with a spreading ridge. The E-W trend is parallel to magnetic lineations in adjacent basins, implying that NER faults are also parallel to the Wharton Ridge. Because the hotspot was thought to be near Wharton Ridge during the formation of NER [*Royer et al., 1991*], a plausible explanation of these features is tensional fault formation at or near the spreading ridge.

An additional argument against recent deformation is that the E-W trend of gravity lineations is mostly inconsistent with predicted relative motions of component plates resulting from intraplate deformation. Moreover, relative motions of the Indo-Australian component plates imply compression at NER, whereas extension appears to have caused the observed horsts and grabens. At the southern NER, convergence between the Australian and Capricorn component plates should be in a WNW-SSE direction (Fig. 1) [*Royer and Gordon, 1997*]. At the northern NER, NW-SE convergence between the Indian and Australian components plates is predicted. In between these two predicted convergence zones is the diffuse triple junction, a region that may be complicated by intersecting stress fields. Although the E-W gravity gradient lineations are parallel to faults and folds formed by N-S compression between the Indian and

Capricorn plates in the Central Indian Basin [*Bull and Scrutton, 1990*], the latter features are found in a zone with much less latitude range than the E-W lineations on NER. In sum, the predicted trends of most plate motions are inconsistent with the observed structural trends within NER and none of the diffuse convergent boundaries should form extensional faults with the observed consistent trend all along the NER.

It is thought that the NER hotspot was near the Wharton spreading ridge because of the close correspondence between seafloor and NER edifice ages [*Royer et al., 1991*]. This close association can also explain our observations. If the NER hotspot was near the spreading ridge, this explains the pervasive extensional faulting as well as the discrepancy between the volcanic propagation rate of the ridge and spreading rates in adjacent basins. With repeated, small, southward ridge jumps, pieces of NER formed on the Antarctic plate would have been added to those formed on the Indian plate, lengthening the ridge beyond that expected simply from northward drift and giving a larger apparent propagation rate. Moreover, repeated small ridge jumps would give the appearance of a linear age progression with coarse age sampling. This hypothesis fits with a trend that more detailed studies of magnetic lineations have defined smaller southward ridge jumps within NER [*Krishna et al., 1999; Desa et al., 2009*]. Unfortunately, it is currently impossible to confirm this hypothesis with magnetic anomalies alone because magnetic data are sparse in the region and anomalies over NER are difficult to interpret [*Krishna et al., 1999; Desa et al., 2009*].

Small ridge jumps could also account for the observed extensive faulting by accreting to the Indian plate pieces of highly faulted NER, formed near the spreading ridge axis, and thus explaining the widespread observed E-W horsts and grabens. Close proximity of the spreading ridge and hotspot can also explain the consistent trend of extensional features because modeling of plume-ridge interaction indicates that the trend of the maximum tensional stress remains perpendicular to the spreading ridge at low hotspot-ridge separations [*Mittelstaedt and Ito, 2005*]. Indeed, this idea fits with the idea that northern NER was formed farther from the spreading ridge, possibly explaining why less E-W lineations are found there. Nevertheless, prominent E-W canyons and troughs are found in the northern NER, implying that even this part of the ridge was formed close to the spreading ridge. Perhaps ridge jumps were fewer and larger in northern NER.

The mechanism of multiple small ridge jumps has been has been proposed for the evolution of the Amsterdam-St. Paul Plateau, a feature located at the SEIR, near NER, that has a similar morphology to the southern NER [*Courrèges et al., 2009; Courrèges, E., et al., "Evolution of ridge segmentation on the St-Paul & Amsterdam Plateau since 10 Ma, in the context of ridge-hotspot interaction," submitted to Geophysical Journal International, 2010*]. If this small ridge jump hypothesis is correct for the NER, it implies that the source of hotspot volcanism was never far from the Wharton Ridge.

Acknowledgements: The authors are indebted to Captain Tom Desjardins, the crew, and technicians of the R/V *Roger Revelle* for their efforts on cruise KNOX06RR. We thank Walter H. F. Smith for advice on satellite gravity data. This project was supported by grants OCE-0550743 and OCE0549852 from the National Science Foundation.

References

Bull, J. M., and R. A. Scrutton (1990), Seismic reflection images of intraplate deformation, central Indian Ocean, and their tectonic significance, *J. Geol. Soc. London, 149*, 955-966, doi:10.1144/gsjgs.149.6.0955.

Courrèges, E., I. Pessanha, M. A. Maia, M. Patriat, W. R. Roest, V. Brandon, and J. Royer (2009), Ridge jumps, segments evolution and accretion rate variations on the St. Paul-Amsterdam Plateau in a context (as a result?) of ridge-hotspot interaction, *EOS, Trans. AGU, 90* (52), abstract V41C-2197.

Curray, J. R., and T. Munasinghe (1989), Timing of intraplate deformation, northeastern Indian Ocean, *Earth Planet. Sci. Lett., 94*, 71-77.

Delescluse, M., and N. Chamot-Rooke (2007), Instantaneous deformation and kinematics of the India-Australia plate, *Geophys. J. Int., 168*, 818-842, doi:10.1111/j.1365-246X.2006.03181.x.

Desa, M., M. V. Ramana, and T. Ramprasad (2009), Evolution of the Late Cretaceous crust in the equatorial region of the Northern Indian Ocean and its implication in understanding the plate kinematics, *Geophys. J. Int. 177*, 1265-1278, doi:10.1111/j.1365-246X.2009.04096.x

Duncan, R. A. (1991), Age distribution of volcanism along aseismic ridges in the eastern Indian Ocean, *Proc. ODP, Sci. Res., 121*, 507-517, doi:10.2973/odp.proc.sr.121.164.1991.

Gopala Rao, D., K. S. Krishna, and D. Sar (1997), Crustal evolution and sedimentary history of the Bay of Bengal since the Cretaceous, *J. Geophys. Res., 102*, 17,747-17,768.

Gradstein, F. M., J. Ogg, and A. Smith (2004), *A Geologic Time Scale*, Cambridge University Press, Cambridge, UK.

Krishna, K. S., J. M. Bull, and R. A. Scrutton (2009), Early (pre-8 Ma) fault activity and temporal strain accumulation in the central Indian Ocean, *Geology, 37*, 227-230, doi:10.1130/G25265A.1.

Krishna, K. S., D. Gopala Rao, M. V. Ramana, V. Subrahmanyam, K. V. L. N. S. Sarma, A. I. Pilipenko, V. S. Shcherbakov, and I. V. Radhakrishna Murthy (1995), Tectonic model for the evolution of oceanic crust in the northeastern Indian Ocean from the Late Cretaceous to the early Tertiary, *J. Geophys. Res., 100*, 20,011-20,024.

Krishna, K. S., D. Gopala Rao, L. V. Subba Raju, A. K. Chaubey, V. S. Shcherbakov, A. I. Pilipenko, and I. V. Radhakrishna Murthy (1999), Paleocene on-spreading axis hotspot volcanism along the Ninetyeast Ridge: An interaction between the Kerguelen hotspot and the Wharton spreading center, *Proc. Indian Acad. Sci., 108*, 255-267.

Luyendyk, B. P. (1977), Deep Sea Drilling on the Ninetyeast Ridge: Synthesis and at tectonic model, in *Indian Ocean Geology and Biostratigraphy*, edited by J. R. Heirtzler, H. M. Bolli, T. A. Davies, J. B. Saunders, and J. G. Sclater, p. 165-187, AGU, Washington, DC.

Mittelstaedt, E., and G. Ito (2005), Plume-ridge interaction, lithospheric stresses, and the origin of near-ridge volcanic lineaments, Geochem. Geophys. Geosys., 6, doi:1029/2004GC000860.

Petroy, D. E., and D. A. Wiens (1989), Historical seismicity and implications for diffuse plate convergence in the Northeastern Indian Ocean, *J. Geophys. Res., 94*, 12,301-12,319.

Pilipenko, A. I. (1996), Fracture zones of the Ninetyeast Ridge area, Indian Ocean, *Geotectonics, 30*, 441-451.

Pringle, M. S., F. A. Frey, and E. E. Mervine (2008), A simple linear age progression for the Ninetyeast Ridge, Indian Ocean: New constraints on Indian plate tectonics and hotspot dynamics, *EOS, Trans. AGU, 89*, abstract T54B-03, 2008.

Royer, J.-Y., and R. G. Gordon, R. G. (1997), The motion and boundary between the Capricorn and Australian plates, *Science, 277*, 1,268-1,274, doi:10.1126/science.277.5330.1268.

Royer, J.-Y., J. W. Peirce, and J. K. Weissel (1991), Tectonic constraints on the hot-spot formation of Ninetyeast Ridge, *Proc. ODP, Sci. Res., 121*, 763-776, doi:10.2973/odp.proc.sr.121.122.1991.

Sandwell, D. T., and W. H. F. Smith (2009), Global marine gravity from retracked Geosat and ERS-1 Altimetry: Ridge segmentation versus spreading rate, *J. Geophys. Res., 114*, 1-16, doi:10.10029/2008JB006008, 2009.

Smith, W. H. F. (1998), Seafloor tectonic fabric from satellite altimetry, *Ann. Rev. Earth Planet. Sci., 26*, 697-738.

Smith, W. H. F., D. T. and Sandwell (1997), Global seafloor topography from satellite altimetry and ship depth soundings: Evidence for stochastic reheating of the oceanic lithosphere, *Science, 277*, 1956-1962.

Veevers, J. J. (1974), Seismic profiles made underway on Leg 22, *Init. Rept. DSDP, 22*, 351-367.

Figure Captions

Figure 1. Location of the Ninetyeast Ridge in the eastern Indian Ocean and areas of diffuse intraplate deformation. Gray shades show regions of expected compressional deformation [*Royer and Gordon, 1997*]. Lighter gray area denotes proposed diffuse triple junction (DTJ). Black arrows show directions of convergence. NER = Ninetyeast Ridge; IN = Indian component plate; CA = Capricorn component plate; AU = Australian component plate; BR = Broken Ridge; SEIR = Southeast Indian Ridge; CLR = Chagos-Laccadive Ridge. Basemap shows satellite-predicted bathymetry [*Smith and Sandwell, 1997*].

Figure 2. Structural interpretation from satellite gravity data. (A) Satellite-predicted bathymetry [*Smith and Sandwell, 1997*] of NER showing KNOX06RR cruise track (red line); DSDP and ODP drill sites (filled circles); and areas of plots D and Figure 3 (boxes). Radiometric ages are given in italics for drill sites [*Pringle et al., 2008*]. (B) Satellite gravity vertical gradient map. Circle shows E-W lineation caused by trough in plot D. (C) Tectonic elements interpreted on gravity gradient. Red and green lines show gradient lineations on the Ninetyeast Ridge; the latter color shows those confirmed by seismic and/or bathymetry data from cruise KNOX06RR. Blue lines show magnetic anomalies and fracture zones. (D) Bathymetry plot from sites NER2-NER3. High-resolution multibeam bathymetry data are plotted around ship tracks (red) with a 250-m contour interval. Low-resolution background bathymetry is predicted from satellite gravity and is plotted with 500 m contours. At center is a deep, E-W trending, graben separating two seamounts. It causes the gravity lineation circled in plots B, C.

Figure 3. (top panels) Bathymetry and satellite gravity gradient features on NER at DSDP Site 214. (left) Multibeam and satellite-predicted bathymetry. Plot conventions as in Figure 2D. (middle, right) Gravity gradient lows (blue shading) and highs (red shading) plotted on bathymetry. Bold red line shows location of seismic section below. (bottom) Seismic profile showing cross-sections of horsts and grabens. Blue shading indicates igneous basement. Sediment ages inferred from nearby DSDP holes [*Luyendyk, 1977*]. Large plus and minus signs show the locations of positive and negative gravity gradient lineations. Red vertical lines show faults.

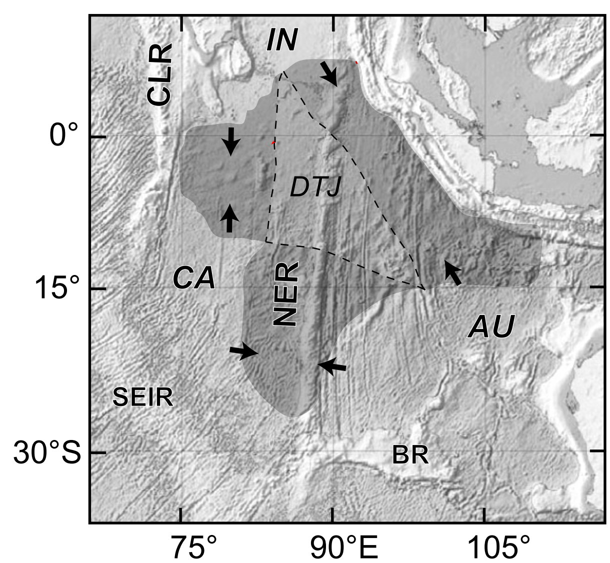

Figure 1

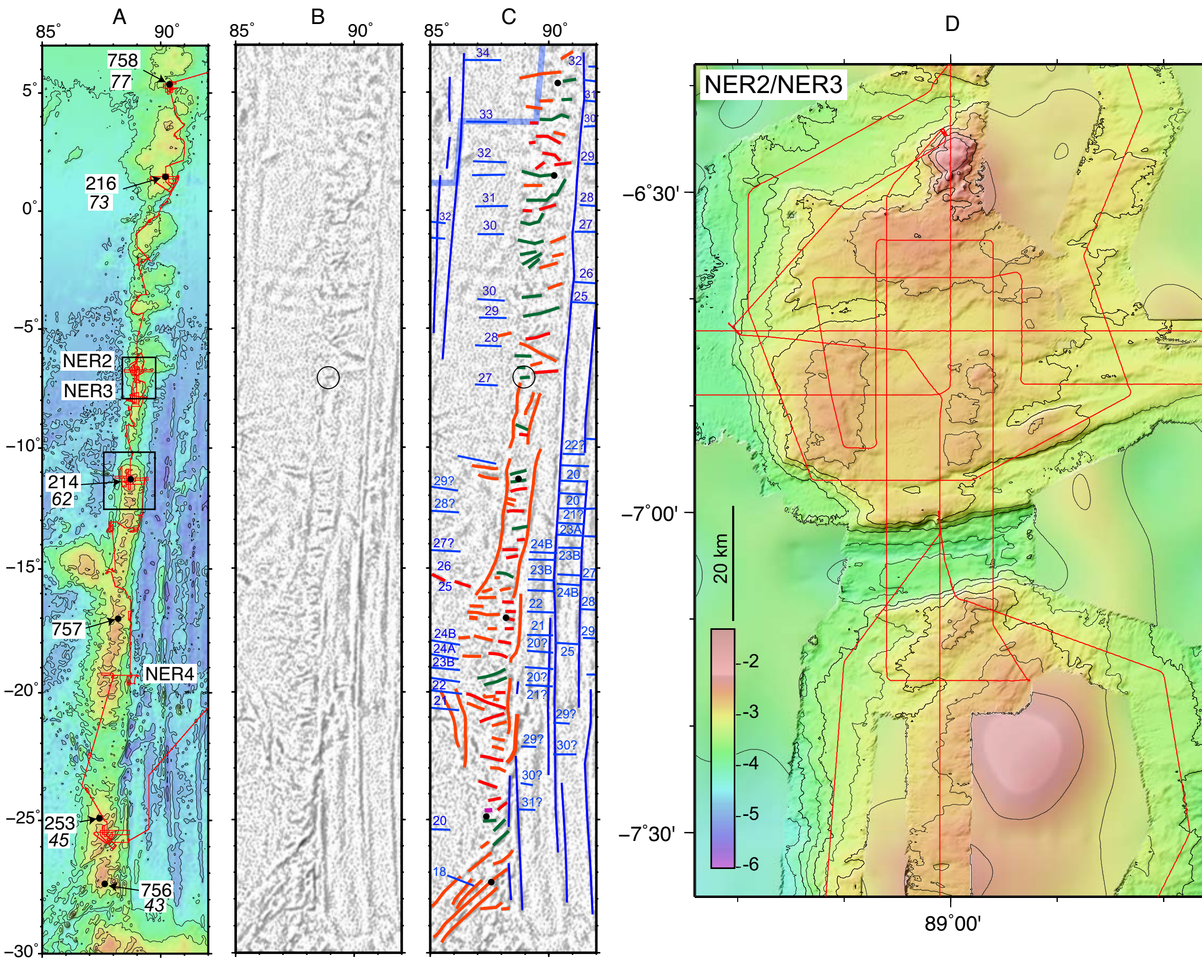
A
B
C
D
85˚
90˚
758
77
216
73
NER2
NER3
214
62
757
NER4
253
45
756
43
5˚
0˚
−5˚
−10˚
−15˚
−20˚
−25˚
−30˚
NER2/NER3
−6˚30'
−7˚00'
−7˚30'
89˚00'
20 km
-2
-3
-4
-5
-6

Figure 2

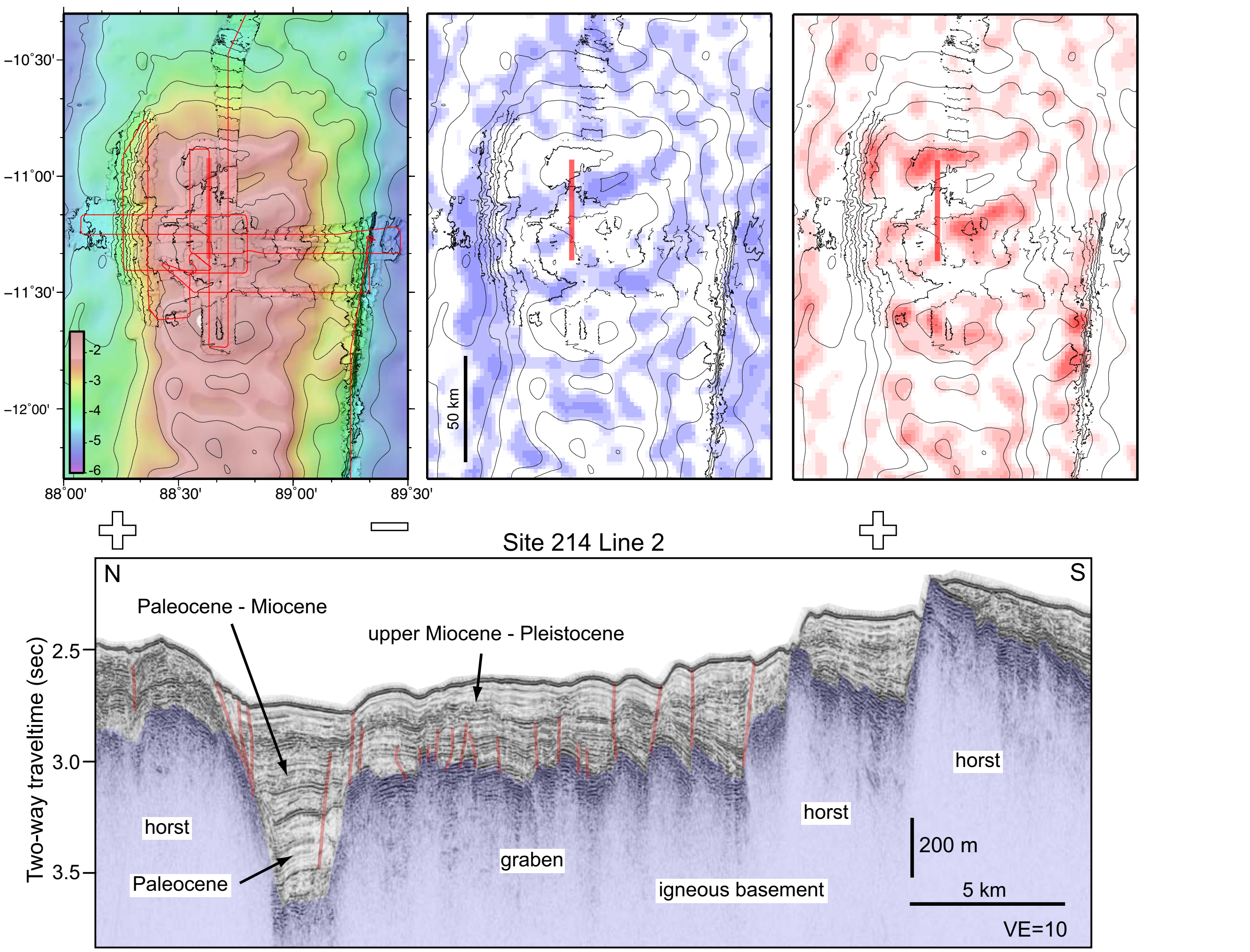

-10°30'
-11°00'
-11°30'
-12°00'
-2
-3
-4
-5
-6
88°00'
88°30'
89°00'
89°30'
50 km
Site 214 Line 2
N
S
Paleocene - Miocene
upper Miocene - Pleistocene
Two-way traveltime (sec)
2.5
3.0
3.5
horst
Paleocene
graben
igneous basement
horst
horst
200 m
5 km
VE=10

Figure 3